

# Water retention parameterization in the WRF model — A sensitivity test

---

## SVALI Deliverable D3.1-1 Report

**BJÖRN CLAREMAR**

**SVALI POSTDOC**

**DEPARTMENT OF EARTH SCIENCES**

**UPPSALA UNIVERSITY**

**JULY/AUGUST 2013**



**UPPSALA  
UNIVERSITET**



## Abstract

Snow accumulation is a complex process and difficult to model due to the uncertainties in precipitation but also in the melting and what happens with the melt water in the snow pack. Additionally the redistribution of the surface snow can be significant in exposed areas. This report investigates the process of the retention and refreezing of melt water and the sensitivity of a number of parameters in the atmospheric model WRF. We use a snow scheme with three layers included in the land surface scheme Noah-MP. The investigated parameters include water holding capacity in the pore space in the snow, heat conductivity of the snow, the maximum snow water equivalent (SWE) handled by the snow scheme and percolation from the lowest snow layer leaving the calculations.

The analysis suggests that the choice of water holding capacity and the heat conductivity can in some cases be important. Although the representation of the deeper snow is more crucial because it gives a hint about how deep the melt water goes. Furthermore, will be counted as internal accumulation or lead to deep runoff following the glacier surface and melt the actual glacier ice? The snow scheme with three layers is not very suitable for deep snow as over glaciers. Thinner layers increases the ability to find ice layers in the snow.

## Introduction

Snow accumulation is a complex process and difficult to model. Firstly the modelled precipitation is associated to large errors (this is one of the most difficult meteorological variables to simulate). The also the partition of snow and rain is also be important (and rather uncertain). Further, the surface sublimation and snow melt must be determined. At the snow surface the wind can also redistribute the snow but with sufficiently large area averages this is of minor importance. However, the melting snow or rain will percolate in the snow pack and will partly be retained in the pores by capillary forces or refreeze on its way down, depending on the cold content in the snow. This means that melting will not necessarily give negative mass balance in the summer but if the melt water in the snow on glaciers percolates down to the firn the annual mass balance will not be correct. The formation of ice lenses and preferential flow or "flow fingers" also complicates the way to model the melt water's way down in the snow pack. It is interesting to model the SMB directly from the atmospheric model but the most important issue for the atmospheric model itself is to find the onset of glacier or ground exposure to the air when the snow is gone, since this effectively changes the surface–air interaction in terms of surface turbulence fluxes and radiation balance.

This report investigates the sensitivity in changing some of the physical parameters in a snow scheme of the atmospheric model WRF. These parameters include water holding capacity in the pore space in the snow, heat conductivity of the snow, the maximum snow water equivalent (SWE) handled by the snow scheme and percolation from the lowest snow layer leaving the calculations.

## WRF Model

The WRF model (Skamarock et al. 2008) is an open source model (<http://www.mmm.ucar.edu/wrf/users/>) widely used in research and is useful in ranges 100 of kilometres down to individual cloud scales of 1–5 km. The model output used in this investigation had horizontal resolution of 16.5 km and the model set-up was basically that of the study by Claremar et al. (2012) but for the WRF3.5 version (not polar WRF). In Claremar et al. (2012) various physics schemes were changed in a sensitivity study. Here we use the Morrison double-moment microphysics scheme (Morrison et al. 2005) and the MYNN2.5 turbulence schemes (Nakanishi and Niino 2006) and the Noah-MP land surface scheme (Niu et al. 2011). Forcing data were from the ERA-Interim re-analysis (Dee et al. 2011). The outer 9 model grid points are omitted to avoid too severe model boundary effects. Fig. 1 shows the model grid and terrain and the glaciers investigated.

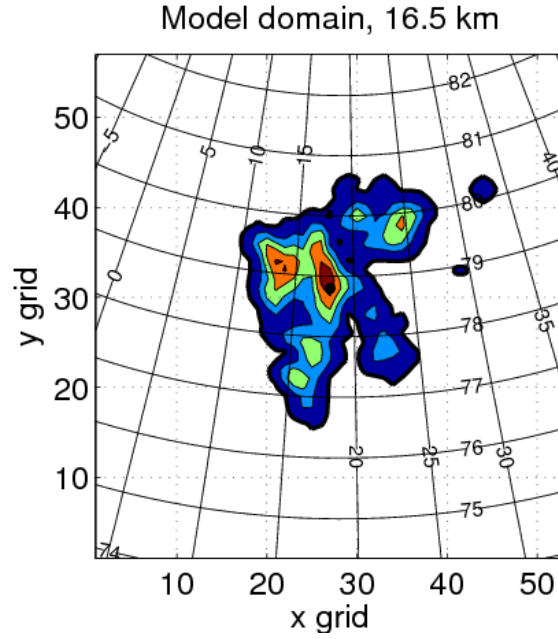


Figure 1 Model domain and Lomonosovfonna marked by dot. Contour lines show elevation with 200 m equidistance.

## Snow scheme

In the WRF model several different land surface schemes can be used. Since the Noah-MP scheme (Niu et al. 2011, Yang and Niu 2003) have several snow layers (3) and liquid water retention and refreezing already implemented this scheme was chosen for this investigation. Snow compaction is accounted for, following Anderson (1976) and Sun et al. (1999). Depending on the snow depth the snow consists of one to three layers. Uppermost layer is limited to 5 cm, the middle one to 20 cm and the lowest is limited by the snow depth and thus can be several meters thick. This thick layer limits the possibility to describe the snow evolution and work with the introduction of more layers was started but cancelled. The architecture of the program code delimited the possibility to do so in the available time frame. We hope this can be done later on in the SVALI project. Snow input is from the ERA-Interim forcing giving up to 50 m of snow. The snow scheme limits it to 2 m SWE.

## Thermal conductivity

The thermal conductivity of the snow,  $k_{snow}$ , is needed to calculate the time evolution of the snow temperature:

$$C_{snow} \frac{\partial T_{snow}}{\partial t} = \frac{\partial}{\partial z} \left( k_{snow} \frac{\partial T_{snow}}{\partial z} \right) + S$$

where the volumetric heat capacity is given by

$$C_{snow} = C_{ice} \theta_{ice} + C_{liq} \theta_{liq}$$

where  $\theta_{ice}$  and  $\theta_{liq}$  stand for partial volume of ice and liquid water and  $C_{ice}$  and  $C_{liq}$  are the specific heat capacity of water and ice at constant volume ( $4.188 \cdot 10^6$  and  $2.094 \cdot 10^6$  J/m<sup>3</sup>/K), respectively.  $S$  is a source/sink term including surface heating and phase changes.

The snow conductivity,  $k_{snow}$ , is parameterized as function of bulk snow density,  $\rho_{snow}$ , for each snow layer. Two different expressions for the snow conductivity are tested, the first one (ref) from Yen (1965):

$$k = 3.2217 \cdot 10^{-6} \rho^2$$

and the other one (condS97) from Sturm et al. (1997):

$$k = 0.138 - 1.01 \cdot 10^{-3} \rho + 3.23 \cdot 10^{-6} \rho^2$$

The difference between the two expressions is shown in Fig. 2. For low densities (new snow) these are very similar but for  $\rho$  higher than  $200 \text{ kg m}^{-3}$  Sturm et al. (1997) gives lower values compared to the Yen (1965).

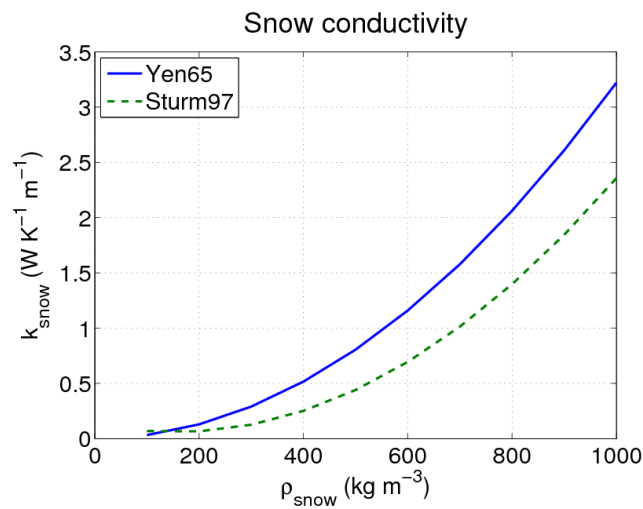


Figure 2. Thermal conductivity in the snow.

### Liquid water in snow pack

Liquid water in the snow is already implemented and dependent on melting, rainfall, the available pore space and the holding capacity, SSI, of the snow pack. The water that do not freeze because of too small amount of cold content in snow layer and is not held by the water holding capacity percolates down to the next layer but can also be prevented from this if the lower layer already is saturated.

The flow from one layer  $i$  is given by:

$$0 < q_{out,i} = (\theta_{liq,i} - SSI \cdot \theta_{pore,i}) dz_i < \theta_{pore,i} - \theta_{liq,i}$$

If the pore space is less than 5% in a layer ( $\rho_{snow} > 850 \text{ kg m}^{-3}$ ) it is considered impermeable. Therefore the percolation is set zero if the actual layer OR the layer below has a pore space below 5%. The lowest snow layer has a free drainage meaning that the snow below is deep and porous. The original code has a constant SSI=0.03. We also test SSI=0.02 (WHC2) which may account for preferential flow that increases the percolation and a relation by Schneider and Jansson (2004) (WHCexp) with higher values and dependent on the porosity (and hence density):

$$\theta_{mi} = 0.0143 \exp(3.3n)$$

where  $n$  is the porosity of the snow and  $\theta_{mi}$  is ratio of irreducible water to the total mass of a snow layer. The flow from one layer is then given by:

$$0 < q_{out,i} = \theta_{liq,i} dz_i - \theta_{mi,i} \cdot m_i < \theta_{pore,i} - \theta_{liq,i}$$

with  $m_i$  is the mass of the mass of the layer.

The changes were only done over the glacier, i.e. only in subroutine module\_sf\_noahmp\_glacier.F (see Appendix).

### Snow initialization

It is of importance that the snow temperature profile is correctly described when starting the model since this will affect the amount of melting, retention and refreezing in the snow later on. The focus of this report is the summer melting but the evolution in the snow during the winter is needed to get the right cold content of the snow. It was decided to start the initialization of the model at the start of the hydrological year, 1 sep 2008. For all runs the two lowest snow levels in the whole domain was given the temperature 0°C and the liquid water content was set to zero. The Fortran code is given in Appendix.

### Snow water equivalent limitations

The original setting of the snow scheme limits the layer to 2 m SWE, which prevents the lowest snow layer to become too thick. The additional water is stored as runoff in the model. In the run init2 the maximum initial SWE is set to 2 m but is then allowed to increase. This is the same as assuming a constant lower horizon of the snow, which is otherwise progressing upwards as new snow is accumulated. To account for a possible layer of ice just below the snow model the simulation init2nro is the same as init2 but the runoff is set to zero in the deep snow layer, allowing liquid water to accumulate and later refreeze. This means that the summer mass balance does not get negative at all as no horizontal flow is accounted for. Thus this is an extreme case because the snow does not disappear from the glacier surface but also gives an indication of the internal accumulation, at least in higher altitudes.

## Results

The different runs performed in this study are summarized in Table 1. They all start on 31 August 2008 and end on 1 September 2009. The analysis focuses on Lomonosovfonna (Fig. 1). The temperature evolution at the snow surface and in the snow layers are shown in Fig. 3 for the reference simulation. The two top snow layers respond fast on surface temperature changes whereas the deep snow layer with centre below 1 m has a negative trend down to -7 °C until July when it abruptly increases to 0°C because of melt water percolation. The first melt event is in the middle of May but then only the top layer reaches 0°C. In middle July all snow is at the melting point but in August the autumn freezing starts but with one melting event around 20 August. The temperature evolution is also seen as a time-depth cross-section in Fig. 4 (keeping in mind that it is based only on 3 snow layers).

Table 1. The simulations performed.

| Run      | Comments  |
|----------|---|
| Ref      | Original Noah-MP snow part of the surface physics scheme                                  |
| condS97  | Conductivity by Sturm et al. (1997)   |
| WHC2     | Water holding capacity set to 0.02 instead of 0.03  |
| WHCexp   | Water holding capacity set to Schneider and Jansson (2004) that is dependent on porosity. |
| Init2    | Initialized to maximum 2 m SWE but not limited during the simulation.                     |
| Init2nro | Same as above but without percolation from deep snow layer.                               |

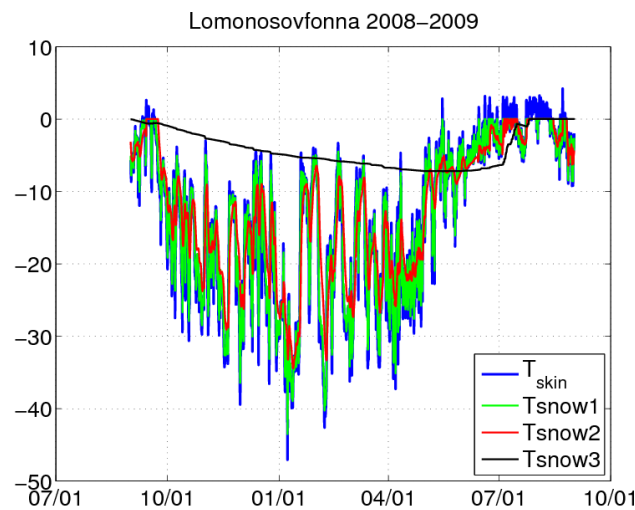
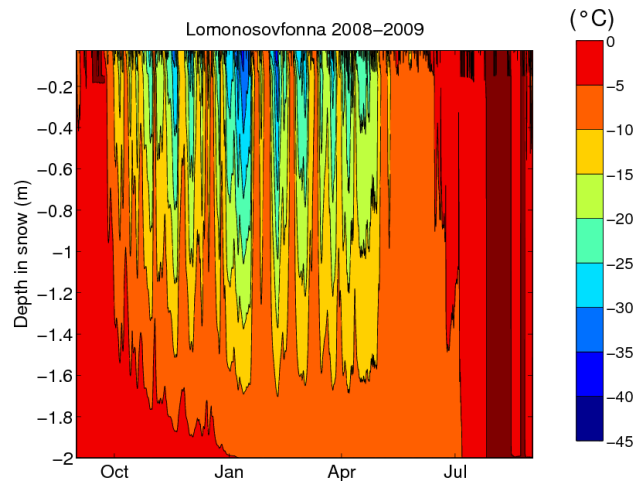


Figure 3. Time series of simulated temperature in the snow layers and at the snow surface.

The autumn part of the simulation serves as a spin-up for temperature and density of the snow layers. In Fig. 5 (Ref) the time evolution of the snow layer densities are shown. The initial density is set to  $300 \text{ kg m}^{-3}$  but changes due to new snow in the top layers ( $100 \text{ kg m}^{-3}$ ) and by compaction due to the weight of overlying snow and aging effects (Anderson 1976; Sun et al. 1999). The deep layer snow stabilizes at circa  $500 \text{ kg m}^{-3}$  already in October and in Fig. 6 this compaction is seen in a reduction of the snow height and is then at least 4 m until the melt season starts. Then liquid water percolates down and contributes to the densification irrespective whether it refreezes or not. In the Ref simulation the melt water percolates in May directly down to the second layer and refreezes instantly and increases the density (Fig. 5, ref) by filling some of the available pore space. No liquid

water is present as seen in Fig. 7. The close-up of the temperature during the melting season (Fig. 8) shows that only the surface snow layer reaches 0°. Deeper down the temperature is still below −4°C. In the end of June the warming of the snow is more evident and liquid water starts to accumulate, first in the top snow layer and later on in the second layer when the water holding capacity is filled in the top layer (Fig. 7). The deeper layers are heated effectively by the water and in the end of July all layers are at the melting point. Liquid water also accumulates in the deep snow layer, increasing the deep layer density as well. At this time the melting starts with full force and according to the simulation this melt is concentrated to two weeks in August reducing the snow layer with 140 mm SWE (Fig. 9) or 0.5 m in snow height (Fig. 6) (also due to compaction from the liquid water).



**Figure 4.** Time-depth cross-section of temperature in the snow. Depth is based on that the deepest layer is about 4 m thick.

The sensitivity test simulations reveal different sensitivities of the changed parameters on the snow characteristics. For snow conductivity the temperature evolution was slower or more inert caused by the lower conductivity for the Sturm et al. (1997) expression. This resulted in somewhat warmer deep layer during the winter but the onset of warming in the summer was neither earlier or delayed compared to the reference (Fig. 8). The total melting from the snow model was however smaller, being circa 110 mm (Fig. 9).

Changing the water holding capacity showed no significant change of the temperature evolution (Fig. 8). Decreasing it to 2 % from 3 % (Fig. 7) had no significant impact, not even on the runoff from the deepest snow model layer. Using the density dependent expression (WHCexp) was somewhat more effective on the density, allowing it to increase above  $550 \text{ kg m}^{-3}$ , and on runoff, reducing it to less than 90 mm (Fig. 9).

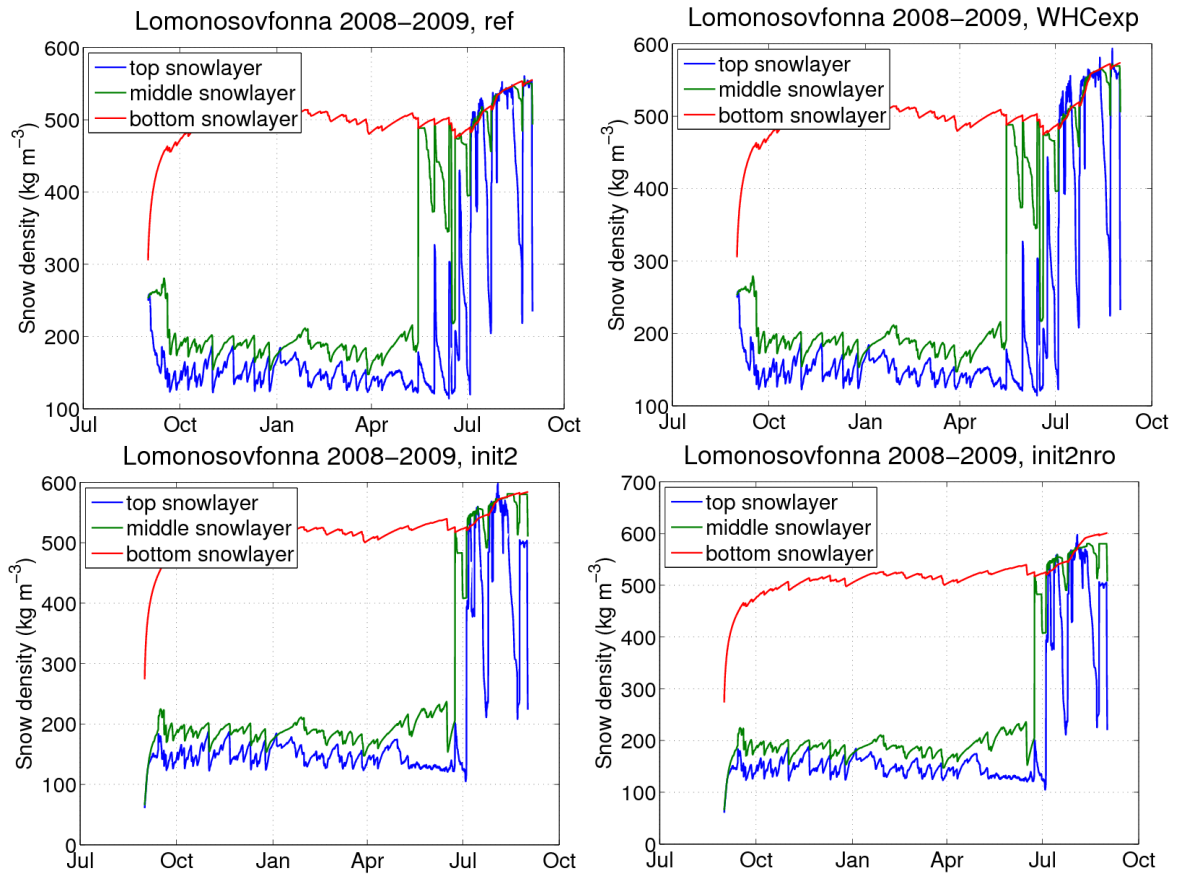


Figure 5. Snow density of the snow layers in the simulations given by the subplot titles.

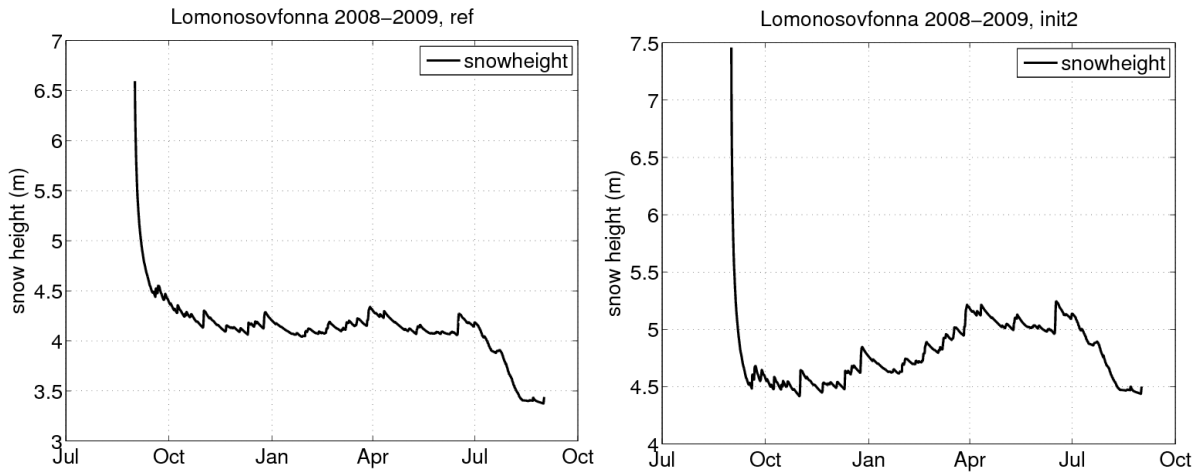


Figure 6. Snow height of the three snow model layers in the simulations given by the subplot titles.

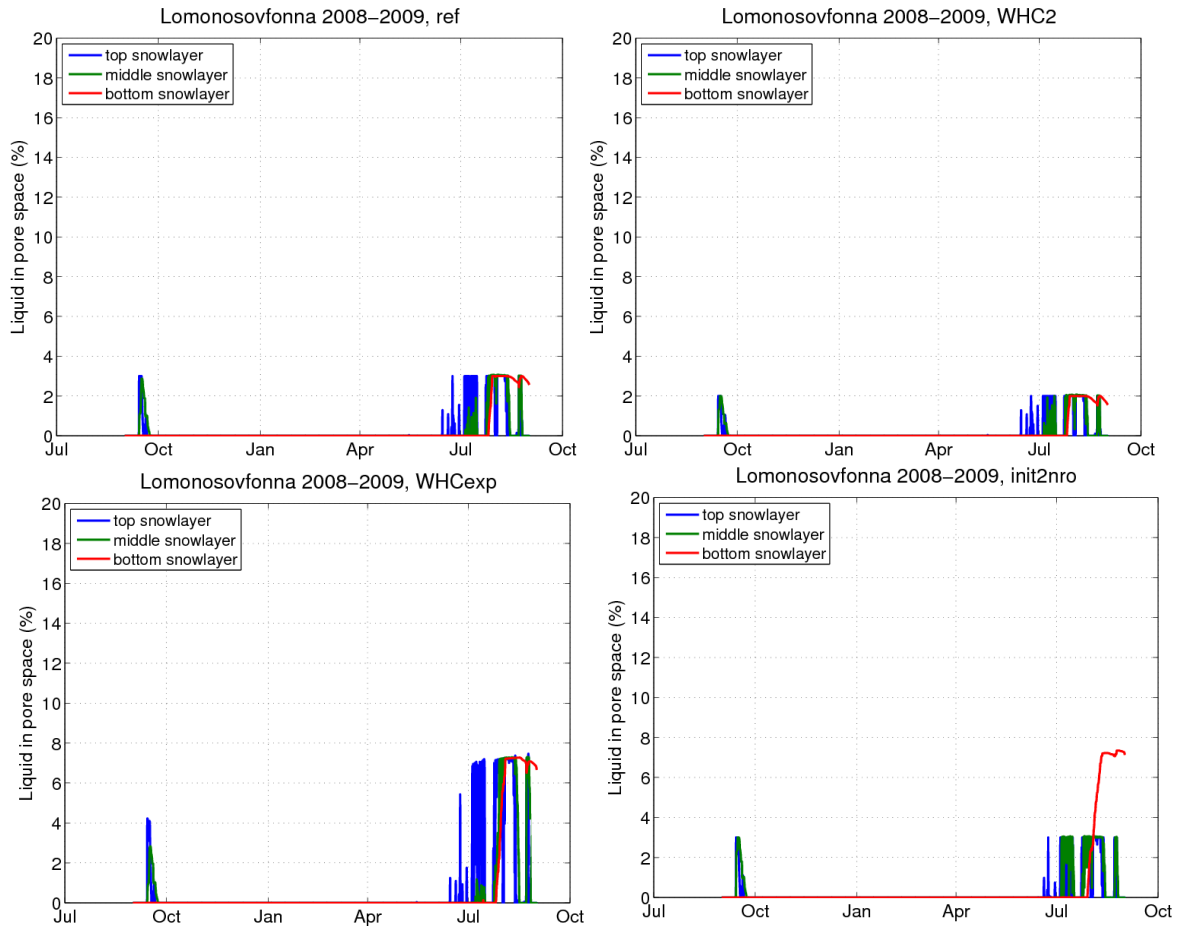
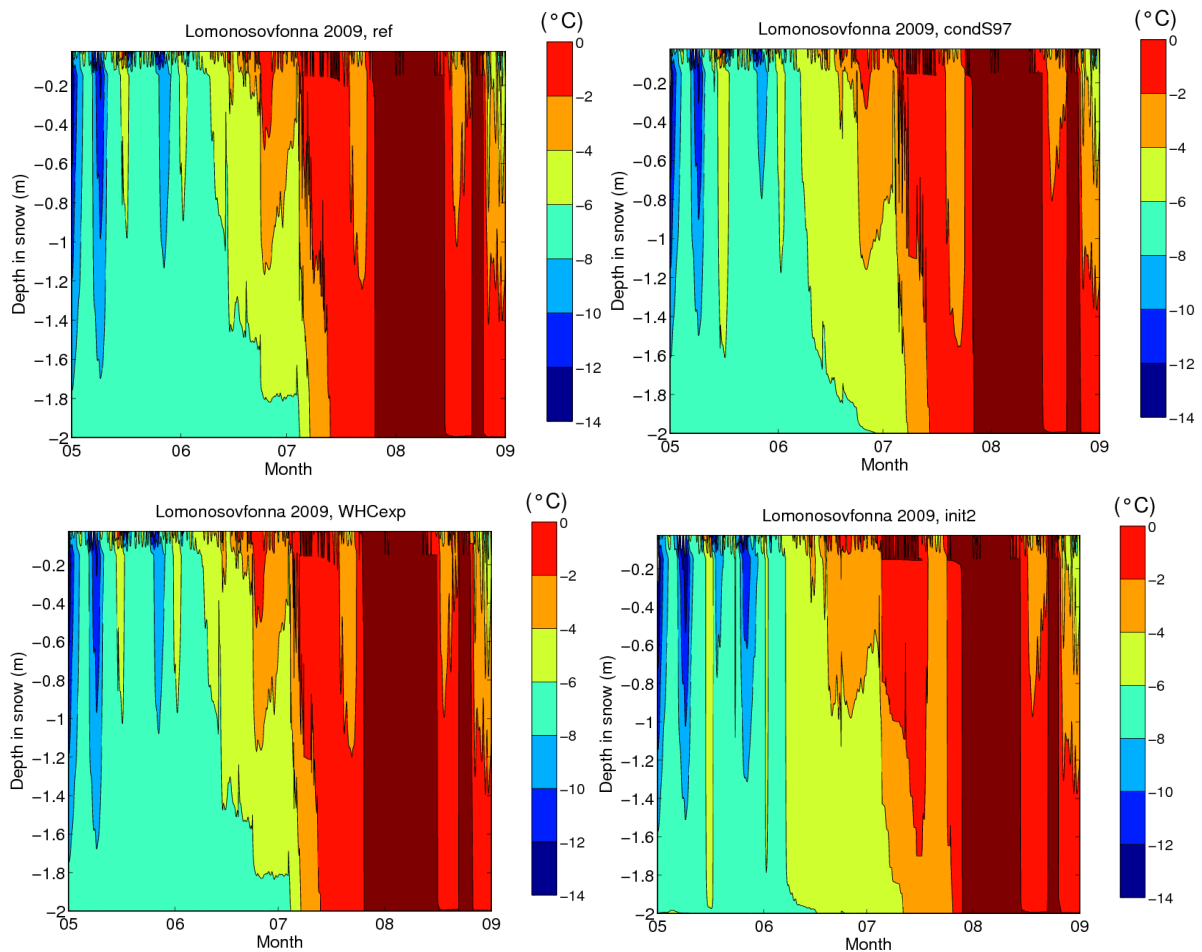


Figure 7. Liquid water content in percent of pore space in the snow layers in the simulations given by the subplot titles.

There are both pros and cons in limiting the snow model to 2 m SWE but by letting the SWE be only limited to 2 m as initial value (can be less if the ERA-Interim forcing data states so) the lower horizon of the snow model is mass conservative for at least the ice and snow. Therefore, as seen in Fig. 9 the precipitation increases the SWE by 650 mm by July and also snow height (Fig. 6) peaking at 5.2 m. The runoff in August is only 70 mm in this case and this can be due to the deeper layer delaying the onset of melting temperature in this layer by a week or so as seen in Fig. 8 (also seen in the density changes in the upper layers in Fig. 5).

If also letting the runoff be limited by a possible glacier surface or an ice-layer that prevents runoff (and assuming small slope and no crevasses in the glacier) the SWE is further increased during the late summer (Fig. 9). The temperature in the snow is not significantly changed compared to the init2 run, but the density becomes larger than  $600 \text{ kg m}^{-3}$  due to the more liquid water in the deep layer, 7% (Fig. 7).



**Figure 8.** Time-depth cross-section of temperature in the snow during the melt season in the simulations given by the subplot titles.

The focus has so far been on the high elevation site Lomonosovfonna. In Fig. 10 the snow height on 15 August is shown in maps for the different sensitivity simulations, when the snow height is the lowest at least for Lomonosovfonna. The reference simulation shows that large parts of the inland Svalbard are covered by at least 3 m of snow, the coast less. The other sub-maps show the differences to the reference for the other simulations (init2nro is compared to init2). Concentrating on the land snow and disregarding the init2 run the changes are within  $-0.2$  m (decrease) and  $0.4$  m (increase) with no obvious systematic dependency on, for instance, height. The init2 run increases the snow height, most at high elevation because of the higher precipitation. The non-runoff run does not significantly change the snow height relative to init2, because of the low melt to accumulation ratio.

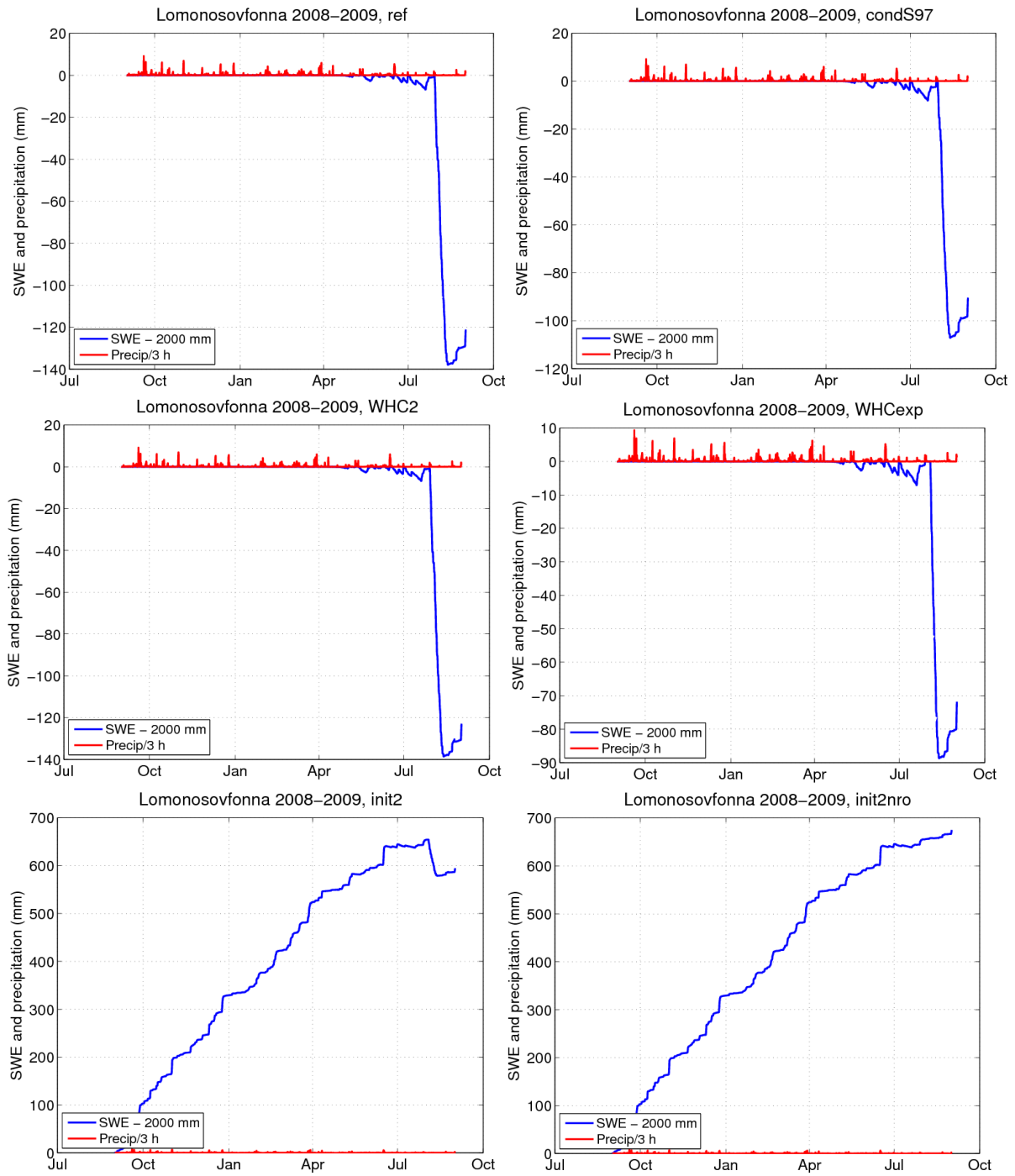


Figure 9. 3-hour precipitation and total SWE in the snow mode layers in the simulations given by the subplot titles.

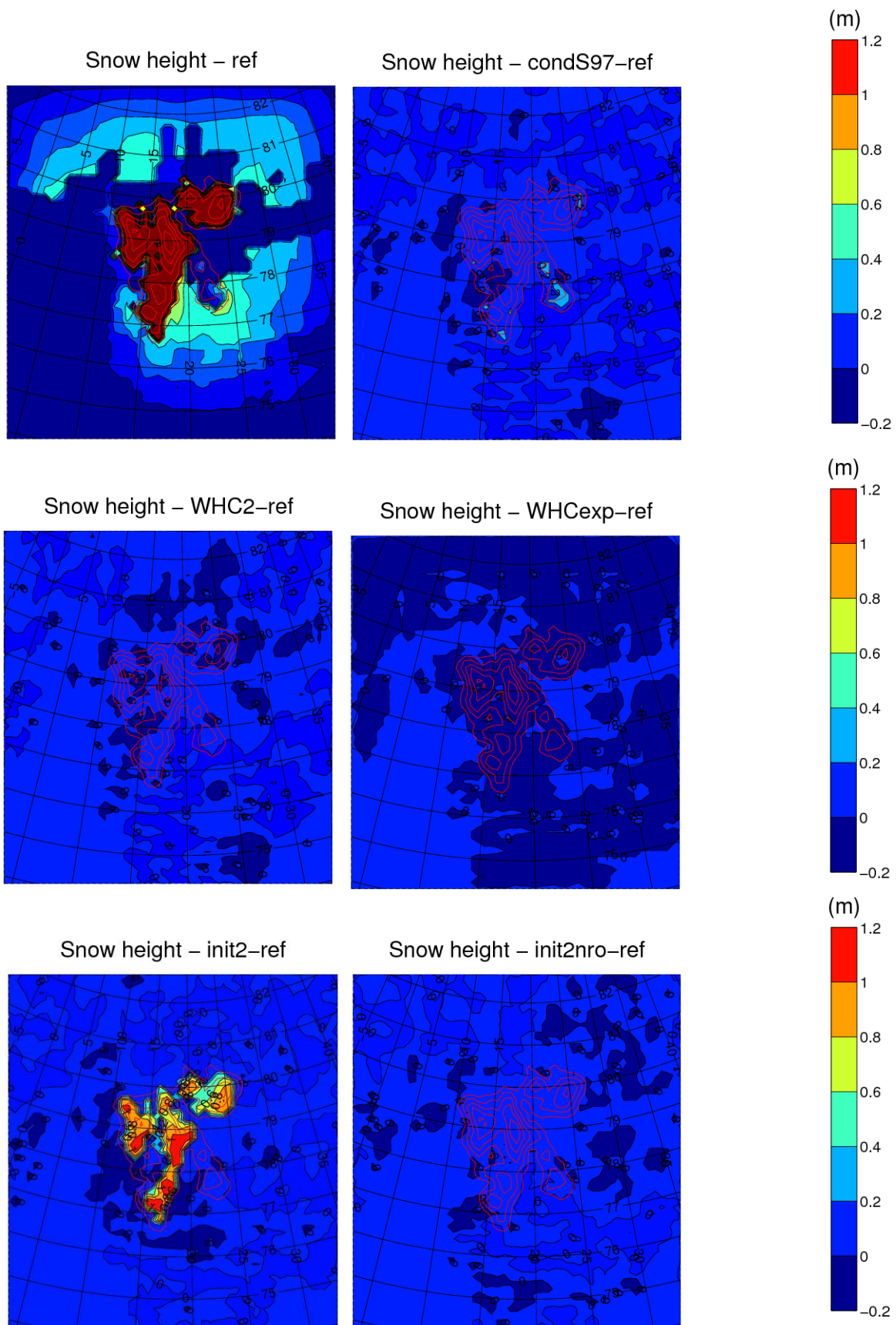


Figure 10. Snow height 15 August 2009 in the simulations given by the subplot titles.

## Discussion and conclusions

Sensitivity simulations by changing the parameters snow conductivity, water holding capacity, snow model thickness and limited deep snow layer runoff have been performed over Svalbard with a focus on the ice sheet Lomonosovfonna. The atmospheric model WRF with the snow scheme part of the land model Noah-MP consisting of three layers was used.

It shows out that most important of the investigated parameters to determine is (at least when the approximate value is known) the water holding capacity since there are a rather broad range of values presented in the literature. The snow heat conductivity can however affect the amount of melting. It is also very important to represent the snow in a good way. Three snow layers are too few to well represent the deep snow evolution. If the snow layers are thin enough the freezing melt water may increase the density so that the layer becomes impermeable ( $\rho_{snow} > 850 \text{ kg m}^{-3}$ ). This is not likely to happen in a 4 m thick snow layer. Unfortunately, increasing the numbers of snow layers was not successful because of the model architecture (difficult also according to the model developers).

Not limiting the snow depth (actually SWE to 2 m) is more physical because the lower horizon of the model is kept constant in the snow pack but decreases the reliability of the model because of the even thicker deep layer. The areas where the snow vanishes from ground or glacier would not suffer from the 2 m limit, unless the snow accumulation during a year exceeds 2 m SWE. Then the initial snow depth should be set lower but above 0 m where there is firn. This is to include the effect of the cold content on the melt water percolation. Runoff from the deep snow layer (or higher up) may be more or less limited by the snow below (because of ice lenses or the glacier itself) and may allow liquid water to be stored above the water holding capacity, forming a slush layer. The lateral runoff can then be parameterized as function of the surface slope (e.g. Zuo and Oerlemans 1996), but the slope was not easily available in the snow model subroutine. Further the lateral flow is complicated by the fact that the snow model is 1-dimensional with no horizontal grid communication. One should also bear in mind the heterogeneity of the snow in a model grid makes it very difficult to account for the ice lenses and the layer characteristics below the snow model.

The simulations were performed in 16.5 km resolution and do not represent Svalbard in a sufficient way in the topography and surface characteristics on the local scale. However, it is believed that the sensitivity study holds for understanding the basics of the uncertainties related to the investigated parameters. The model performance in relation to measurements will be the topic of a manuscript related to SVALI deliverables 3.1-2 and 3.1-5. Input from the measurements in WP 2.3 will also be considered.

### To conclude:

- The Noah-MP snow scheme with three layers is not very suitable for deep snow as over glaciers. Thinner layers increases the ability to find ice layers in the snow.
- Information of the layer directly below the snow model is needed to determine what happens to the melt water in the end.
- Determining the correct water holding capacity and the heat conductivity in the snow can be important under some circumstances.
- Validation/tuning of the snow model to measurements are needed.

## Acknowledgements

Veijo Pohjola and Anna Rutgersson at Uppsala University are thanked for input and discussions. So are Carl Bøggild at university center in Greenland, Guðfinna Aðalgeirsdóttir at University of Iceland and Ruth Mottram at DMI. The work was funded by the Nordic council of ministers (SVALI, [www.ncoe-svali.org](http://www.ncoe-svali.org)).

## References

- Anderson, E.A. (1976). A point energy mass balance model of a snow cover. *NOAA Tech. Rep. NWS 19*, 150 pp., Off. of Hydrol., Natl. Weather Serv., Silver Springs, Md.
- Claremar, B., Obleitner, F., Reijmer, C., Pohjola, V., Waxegård, A. et al. (2012). *Applying a Mesoscale Atmospheric Model to Svalbard Glaciers*. *Advances in Meteorology*. 321649
- Dee, D. P., Uppala, S. M., Simmons, A. J., Berrisford, P., Poli, P., et al. (2011). *The ERA-Interim reanalysis: configuration and performance of the data assimilation system*. *Q.J.R. Meteorol. Soc.*, **137**: 553–597. doi: 10.1002/qj.828
- H. Morrison, J. A. Curry, and V. I. Khvorostyanov (2005), A new double-moment microphysics parameterization for application in cloud and climate models. Part I: Description. *J. Atm. Sci.*, vol. 62, no. 6, 1665–1677.
- Nakanishi, M. and Niino H. (2006), An Improved Mellor–Yamada Level-3 Model: Its Numerical Stability and Application to a Regional Prediction of Advection Fog, *Boundary-Layer Meteorol.*, vol. 119, no. 2, pp. 397–407.
- Niu, G.-Y., Yang Z.-L., Mitchell K.E., Chen F., Ek, M.B., et al 2011. The community Noah land surface model with multiparameterization options (Noah-MP): 1. Model description and evaluation with local-scale measurements. *J. Geophys. Res.*, 116, D12109, doi: 10.1029/2010JD015139.
- Schneider, T. and Jansson, P 2004. Internal accumulation in firn and its significance for the mass balance of Storglaciären, Sweden. *J. Glaciol.*, 50, 25–34.
- Sturm, M., Holmgren, J., König, M., and Morris, K. 1997. The thermal conductivity of seasonal snow, *J. Glaciol.*, 43, 26–41.
- Sun, S., Jin, J.M., and Xue, Y 1999. A simple snow-atmosphere-soil transfer model. *J. Geophys. Res.*, 104, 19,587–19,597, doi: 10.1029/1999JD900305.
- Wilson, A. B., D. H. Bromwich, K. M. Hines (2011): Evaluation of Polar WRF forecasts on the Arctic System Reanalysis domain: Surface and upper air analysis. *J. Geophys. Res.*, **116**, D11112, doi: 10.1029/2010JD015013
- Yang Z.-L. and G.-Y. Niu 2003. The versatile Integrator of surface and atmospheric processes (VISA) part 1: Model description. *Global Planet. Change*, 38, 175–189, doi: 10.1016/S0921-8181(03)00028-6.

Yen YC. 1965. Heat transfer characteristics of naturally compacted snow. US Army Cold Regions Research and Engineering Laboratory, Research Report 166, Hanover, NH, 9 pp.

Zuo, Z., and Oerlemans, J. 1996. Modelling albedo and specific balance of the Greenland ice sheet: calculations for the Søndre Strømfjord transect. *J. Glaciol.*, 42, 305–317.

## Appendix: Model code

### Snow initialization

The snow initialization is done in the file phys/module\_sf\_noahmpdrv.F. The snow temperature is set to 0° in the two lowest layers over glacier ice (IVGTYP (I,J)==ISICE .AND. XICE(I,J) <= 0.0). Since the subroutine snow\_init do not include these parameters they are included in the call. Also the deep soil temperature, TMN, was included if one wants to include a dependency on this variable on the snow temperature. Below, the lines affected by the changes are shown.

```
CALL snow_init ( ims , ime , jms , jme , its , itf , jts , jtf , NSNOW , &
&              NSOIL , zsoil , snow , tgxy , snowh ,      &
&              zsnsoxy , tsnoxy , snicexy , snliqxy , isnowxy , &
&              IVGTYP , ISICE , XICE , TMN)                !BC
```

```
SUBROUTINE SNOW_INIT ( ims , ime , jms , jme , its , itf , jts , jtf ,      &
&                    NSNOW , NSOIL , ZSOIL , SWE , TGXY , SNODEP ,          &
&                    ZSNSOXY , TSNOXY , SNICEXY ,SNLIQXY , ISNOWXY ,      &
&                    IVGTYP , ISICE , XICE, TMN) !BC
```

```
!BC130619
```

```
INTEGER, INTENT(IN)                                :: ISICE
```

```
INTEGER, DIMENSION( ims:ime, jms:jme ),INTENT(IN):: IVGTYP
```

```
REAL, DIMENSION(ims:ime,jms:jme), INTENT(IN)      :: XICE !sea ice fraction
```

```
IF(ISNOWXY(I,J) == -NSNOW) THEN                    !BC130620
```

```
    IF(IVGTYP(I,J)==ISICE .AND. XICE(I,J) <= 0.0) THEN !BC130620
```

```
        TSNOXY(I,0,J) = 273.15                       !BC130620
```

```
        TSNOXY(I,-1,J) = 273.15                      !BC130620
```

```
    END IF                                           !BC130620
```

```
END IF
```

### Irreducible water (water holding capacity)

In module\_sf\_noahmp\_glacier.F

```
THMI (J)      = 0.0143*exp(3.3*EPORE(J))
```

```
!QOUT = MAX(0.,VOL_LIQ(J)*DZSNSO(J)-THMI(J)*SNICE(J)/1000) !WHCexp
```

```
QOUT = MAX(0.,(VOL_LIQ(J)-SSI*EPORE(J))*DZSNSO(J))
```

```
QOUT = MIN(QOUT,(1.-VOL_ICE(J+1)-VOL_LIQ(J+1))*DZSNSO(J+1))
```